Article

Budesonide analogues preserve stem cell pluripotency and delay 3D gastruloid development

Filomena Amoroso[1*], Eduardo Ibello[1*], Federica Saracino[1], Federica Cermola[1], Giovanna Ponticelli[1], Enrica Scalera[2], Francesca Ricci[2], Gino Villetti[2], Gilda Cobellis[3], Gabriella Minchiotti[1], Eduardo Jorge Patriarca[1], Dario De Cesare[1^], Cristina D'Aniello[1^]

[1] Stem Cell Fate Laboratory, Institute of Genetics and Biophysics "A. Buzzati Traverso", CNR
[2] Experimental Pharmacology & Translational Science Department, CorporatePre-Clinical R&D, Chiesi
[3] Department of Precision Medicine, University of Campania Luigi Vanvitelli, Naples, Italy
* Equal contribution as first authors
^ Correspondence: cristina.daniello@igb.cnr.it (CD); dario.decesare@igb.cnr.it (DDC)

Abstract: Small molecules that can modulate or stabilize cell-cell interactions are valuable tools for investigating the impact of collective cell behavior on various biological processes such as development/morphogenesis, tissue regeneration and cancer progression. Recently, we showed that budesonide, a glucocorticoid widely used as anti-asthmatic drug, is a potent regulator of stem cell pluripotency. Here we tested the effect of different budesonide derivatives and identified CHD-030498 as a more effective analogue of budesonide. CHD-030498 was able to prevent stem cell pluripotency exit in different cell-based models, including embryonic stem-to-mesenchymal transition, spontaneous differentiation and 3D gastruloid development, and at lower doses compared to budesonide.

Keywords: drug toxicity; budesonide analogues; stem cells; pluripotency exit; 3D gastruloids.

1. Introduction

Extrinsic cues generated by the cell-cell interactions control the cell identity/phenotype of mammalian cells, including their morphology, proliferation, and motility. Indeed, a reversible/dynamic process of stabilization and destabilization of intercellular interactions is crucial for normal embryo development and regeneration of adult tissues following injury. The impact of homotypic and heterotypic cell interactions on cell behaviour is studied in helpful models of tissue regeneration including healing of injured skin [1, 2] , fibrocartilage [3], bone [4, 5] and muscle [6-8], as well as in models of tumorigenesis as the epithelial-to-mesenchymal transition (EMT) involved in cancer progression [9, 10]. Of note, the embryonic organoids generated from aggregates of pluripotent (mouse and human) stem cells, including gastruloids and blastoids, are emerging models to study collective cell behaviour during early embryogenesis [11, 12].

Growth factors and small molecules able to modulate the cell-cell physical contacts could represent useful tools to identify the underlying molecular mechanisms. Recent reports shed light on a previously unrecognised activity of budesonide, a glucocorticoid that is largely used as a potent anti-asthmatic drug [13, 14]. Budesonide counteracts exit from pluripotency that occurs either spontaneously upon removal of undifferentiating factors (LIF, CHIR99021, PD0325901) or is induced by L-proline supplementation (esMT) in 2D ESC culture, promoting cell-cell adhesion and reducing the phenotypic and molecular heterogeneity of ESCs. Budesonide also prevents ESCs aggregates to self-organize and generate elongated 3D gastruloids, a process that is still poorly characterized. Specifically, budesonide promotes compaction of 3D ESCs aggregates, which eventually fail to break symmetry, at least in part by favoring cell-cell interaction and preventing cell migration.

 doi:10.20944/preprints202305.2155.v1

This activity of budesonide is unique among the classical glucocorticoids and it is independent of the Glucocorticoid Receptor (GR) [13].

Here, in the search for more active small molecules to investigate ESCs self-organization properties, we assessed the effects of structural analogues of budesonide on 2D and 3D ESCs cultures and identified a new compound, named CHD-030498, which favours the maintenance of pluripotency state and prevents symmetry breaking and 3D gastruloids elongation with higher efficacy compared to budesonide.

2. Materials and Methods

Cell cultures and treatments

The embryonic stem cell lines: wild-type E14Tg2a (E14), shNT (control) and sh*Nr3c1* KD were used throughout this study. ESCs were grown in FBS/LIF in standard conditions as previously described [13, 19], using high glucose DMEM (Invitrogen, Life Technologies), 15% FBS (Euroclone), 2 mmol/L glutamine, and penicillin/streptomycin (100 U/mL; GIBCO). All the experiments were performed between the 10^{th} and the 25^{th} cell passage. For all cell lines Mycoplasma-free state is routinely (twice/year) tested by PCR-based assay. Budesonide, fluticasone and BA-GCs compounds (provided by CHIESI Farmaceutici) were dissolved in DMSO at a concentration of 10 mM and used at concentration range between 10^{-5} and 10^{-10} M.

Cytotoxicity, Proliferation and apoptosis assays

To assess the cytotoxic effects of BA-GCs, ESCs were plated at $1x10^4$ cells/cm^2, in triplicate, on gelatin-coated 96-multiwell plates (Corning) ± increasing concentrations (10^{-10}, 10^{-9}, 10^{-8}, 10^{-7}, 10^{-6}, 10^{-5} M) of the compounds or with the solvent (DMSO) alone as control. Halofuginone (HF; nM concentrations) was used as additional control [15]. After 24 hrs in culture, cells were incubated with CCK-8 (10 µl; Dojindo Laboratories, Kumamoto, Japan) for 24 hrs, as previously described [14]. The absorbance, which is directly proportional to the number of living cells, was measured at 450 nm using the spectrophotometer Synergy H1 Microplate Reader (BioTek).

For cell proliferation, we used the 5-ethynyl-2'-deoxyuridine (EdU; Invitrogen) assay. Briefly, $1x10^4$ ESCs /cm^2 were plated on gelatin-coated plates (Corning), and treated with the different compounds. Two or three concentrations among the highest (10^{-5}, 10^{-6} and 10^{-7} M) were used for each compound. CHD-030498 was used at 5, 2.5, 1 and 0.1 µM, since at 10 µM showed a toxic effect. DMSO was used as a control. After 24 hrs in culture cells were incubated with EdU (10 µM) overnight. ESCs were then detached with trypsin and the EdU staining protocol was performed, following manufacturer's instructions. Briefly, cells were fixed for 10 minutes at room temperature (RT). After washing and permeabilization with a saponin-based buffer for 10 minutes at RT, cells were stained with a cocktail solution (EdU kit), containing the 488 fluorofore. After an incubation period of 30 minutes in the dark, cells were washed and analysed by FACS (Aria II cell sorter Becton Dickinson). One well of untreated cells (UT) was left without EdU treatment as negative control.

Apoptosis was analysed using the Annexin V/Propidium iodide (PI) staining (Dojindo Laboratories, Kumamoto, Japan). Briefly, $1x10^4$ ESCs /cm^2 were seeded on gelatin-coated plates (Corning) and treated with the different compounds (10^{-5}, 10^{-6} and 10^{-7} M), as above. ESCs were treated ± the solvent (DMSO) as control. After 48 hrs in culture, both adherent and suspension cells were collected following standard procedures, and apoptosis was measured by Annexin V/Propidium iodide (PI) staining, following manufacturer's instructions. Briefly, cells were counted and resuspended at final concentration of $1x10^6$ cells /ml in Annexin V Binding Solution, containing both Annexin V and PI, for 15 minutes at RT in the dark. DMSO-treated cells that not stained with Annexin V/PI were used as a negative control. Then, the staining solution was diluted 1:5 and the samples were analysed by FACS (Canto, Becton Dickinson).

 doi:10.20944/preprints202305.2155.v1

esMT/MesT

Embryonic stem cell to mesenchymal-like transition (esMT) was performed as previously described [14, 16]. Briefly, ESCs were plated at low density (300 cells/cm^2) on gelatin-coated plates and treated ± proline (250 μM), ± the compounds supplemented at different final concentrations (from 10^{-11} to 10^{-5} M). Budesonide and fluticasone were used at 10 μM as a positive and a negative control, respectively. The dose-dependent effect of CHD-030498 was analysed in detail at 10, 7.5, 5, 2.5 and 1 μM. For mesenchymal-like to embryonic stem cell transition (MesT) freshly generated proline-induced mesenchymal-like cells (PiCs) were plated at low density (300 cells/cm^2) and treated ± proline (250 μM), as controls, and ± the compounds, at concentrations ranging from 10^{-5} to 10^{-7} M. At day 5 the colonies resulting from either esMT or MesT were fixed and stained with a solution of PBS1x/6% glutaraldehyde/0.15% crystal violet, and the frequency of domed *versus* flat colonies were scored as a quantitative readout of the phenotypic transition as previously described [14, 16].

Pluripotency exit

ESCs were cultured in FBS/2i/LIF medium for 3 days and then shifted to either FBS alone, FBS + budesonide (10 μM), fluticasone (10 μM), CHD-030498 (10, 5, 2.5 and 1 μM) or maintained in FBS/2i/LIF as a control for additional 4 days. The resulting colonies were fixed and stained with a solution of PBS1x/6% glutaraldehyde/0.15% crystal violet and the frequency of flat colonies was scored [13].

Gastruloid formation assay

Gastruloids were generated as described [13, 18, 19]. ESCs were seeded at 2.5–3.0 × 10^2 cells/well. CHIR99021 (3 μM) was added between 48 and 72 hrs. From 72 hrs onwards, medium was refreshed every day. Budesonide (1 and 10 μM), CHD032201 (1 and 10 μM) and CHD-030498 (10, 1, 0.5, 0.25 and 0.125 μM) were added either during the first 48 hrs or for 120 hrs. Gastruloids were imaged using EVOS. Aggregates diameter at 48 hrs was analysed using Image J 1.46r software (https://imagej.nih.gov/ij/). Elongation index was calculated using ImageJ-Fiji (BIOP plugin).

RNA extraction and Real time PCR

Total RNA was extracted using Trizol (Life Technologies), and reverse transcribed using the High Capacity cDNA reversion transcription kit (Applied Biosystems). Real-time PCR was performed using SYBR Green PCR master mix (FluoCycle IITM SYBR, Euroclone) on the BioRad CFX qPCR machine. The experiments were performed in technical triplicate and in biological duplicate. The primer sequences are reported in **Table 1**.

Table 1

Gene	Primer Forward	Primer Reverse
N-Cad	AGCGCAGTCTTACCGAAGG	TCGCTGCTTTCATACTGAACTTT
Mmp2	TTCCCTAAGCTCATCGCAGACT	CACGCTCTTGAGACTTTGGTTCT
T	GAACCTCGGATTCACATCGT	TTCTTTGGCATCAAGGAAGG

Immunofluorescence

Immunofluorescence on gastruloids was performed as described [18, 20]. For staining with BRACHYURY, gastruloids were first washed at RT with PBS (3×, 10 min), PBS/10% FBS/0.5% Triton X-PBSFT (3×, 10 min), and then with PBSFT (1 hr, 4°C), and incubated with antibodies (48 hrs, at 4°C) on a low-speed orbital rocker. Confocal images were obtained on a Nikon A1 microscope. The AF6000 (Leica Microsystems) and NIS Element C (Nikon, Tokyo) software were used for image acquisition/elaboration.

 doi:10.20944/preprints202305.2155.v1

3. Results

3.1 Effect of budesonide-analogues glucocorticoids (BA-GCs) on ESC proliferation

To search for budesonide analogues, we tested a few compounds having the basic 4-ring steroid backbone and different residues in position 6, 9, 16 and 17 (**Figure 1A**). For instance, compound CHD-030498 (MW 521,65) contains a fluor atom, instead of hydrogen, in position 6 (R1) and 9 (R2), such as fluticasone. Moreover, it contains a 17-(2-hydroxyacetyl) residue in position 17 (R3), and a pentacyclo structure involving positions 16 and 17 (R4), such as budesonide (**Figure 1A**). Thus, CHD-030498 displays structural features of both fluticasone and budesonide. We first tested the effect of the selected compounds, hereafter named budesonide-analogue glucocorticoids (BA-GCs), on embryonic stem cells (ESCs) by using a CCK-8 sensitive colorimetric assay (**Figures 1B** and **Supplementary Figure 1A**). Our analysis revealed that: i) halofuginone (HF), a potent inhibitor of prolyl-tRNA synthetase used as a positive control [15], reduced ESC survival in a dose-dependent manner; ii) budesonide did not exert any toxic effects in the same concentration range (1 nM to 10 μM), as fluticasone (**Figure 1B**); iii) CHD-030498 was toxic at the highest concentration (10 μM **Figure 1B**); iv) none of the other BA-GCs assayed, including CHD-030614, CHD-032201, CHD-031019, CHD-026409, CHF6162.00 and CHD6183.00, affected ESCs viability/proliferation at any concentrations (**Supplementary Figure 1A**).

To support these findings, we performed Annexin V/PI apoptosis assay, which allows to distinguish alive (Annexin V^-/PI^-) from dead cells, and discriminate early (Annexin V^+/PI^-) and late (Annexin V^+/PI^+) apoptotic cells, or necrotic cells (Annexin V^-/PI^+). Quantification of the Annexin $V^\pm/PI^\pm$ cell fraction revealed that at 1 μM both budesonide, fluticasone (**Figure 1C**) and most of the BA-GCs assayed (**Supplementary Figure 1B**) did not induce apoptosis and/or necrosis in ESCs (**Figure 1C** and **Supplementary Figure 1B**). Instead, at 10 μM some BA-GCs, including CHD-030614, CHD-031019, CHD-026409, CHF6162.00 and CHD6183.00, induced a 2-fold increase in the fraction of apoptotic cells (**Supplementary Figure 1B**). The fraction of Annexin V^+/PI^+ cells increased significantly from ~20% to ~80%, in the presence of CHD-030498 at 1 and 10 μM, respectively (**Figure 1C**). A cell counting analysis revealed that 10 μM CHD-03049 increased the fraction of trypan blue positive (dead) cells (**data not shown**).

To further validate these data, we assessed the impact of BA-GCs on ESC proliferation by 5-ethynyl-2'-deoxyuridine (EdU) incorporation. The fraction of EdU^+ (proliferating) cells was comparable (ranging around 98%-99%) among the different BA-GCs tested (**Figure 1D** and **Supplementary Figure 1C**), confirming the absence of any toxic effects. Of note, CHD-030498 did not alter significantly ESCs proliferation in a wide concentrations range (100 nM to 5 μM) (**Figure 1D**).

3.2 BA-GCs prevent embryonic stem cell-to-mesenchymal transition (esMT) induction

We then tested the ability of BA-GCs to counteract exit from pluripotency in different 2D culture conditions. First, we analysed the ability of BA-GCs to prevent the transition from naïve to early primed pluripotency induced by proline supplementation (esMT) [16]. Briefly, we performed colony formation assays (CFAs) by plating ESCs at low density on gelatin-coated plates ± proline (250 μM) ± BA-GCs (0,01 nM to 10 μM) (**Figure 2A**). Budesonide and fluticasone were used as positive and negative controls, respectively [13, 14]. Following five days of culture, the cell colonies were fixed, stained and imaged; esMT was evaluated by measuring the fraction of round domed (naïve embryonic) *versus* irregular flat (mesenchymal-like) colonies (**Figure 2A**). The results showed that: i) budesonide, unlike fluticasone, prevented the acquisition of mesenchymal/flat morphology associated with esMT (**Figure 2B**); ii) at 10 μM CHD-030614, CHD-032201, CHD-031019, CHD-026409 and CHF6183.00 inhibited esMT similarly to budesonide (**Figure 2B**); iii) at 1 μM most of the compounds were inactive, whereas CHD-030498 exerted a stronger inhibitory effect, showing ~60% of domed colonies. In line with the results obtained with CCK-8 assay, no colonies were detected in the presence of CHD-030498 at 10 μM (**Figure 2B**). Furthermore,

 doi:10.20944/preprints202305.2155.v1

we analysed the expression of the mesenchymal marker *Mmp2* (matrix metallopeptidase 2) known to be induced by proline [16]. Of note, *Mmp2* upregulation was reduced to a similar extent in the presence of 10 μM budesonide, CHD-030614, CHD-032201, CHD-031019, CHD-026409, and CHF6183.00 (**Figure 2C**). Finally, we performed a dose-dependent assay and confirmed that while CHD-030498 activity was comparable in the 5 to 1 μM range, budesonide activity progressively decreased from 5 to 1 μM (**Figure 2D**).

We then assessed the ability of BA-GCs to drive the reverse process of esMT, named mesenchymal-to-embryonic transition (MesT). Freshly generated proline-induced cells were dissociated and re-plated at low density (300 cells/cm^2) in undifferentiation medium ± proline (250 μM), ± BA-GCs added at concentrations ranging from 0.1 μM to 10 μM (**Supplementary Figure 2A**). At day 4, the frequency of reverted (domed-shaped) colonies was scored as a parameter of MesT transition. Proline addition reduced the fraction of domed colonies compared to untreated cells (**Supplementary Figure 2A**), whereas budesonide (10 μM) efficiently counteracted the acquisition of the mesenchymal phenotype, as previously reported [17] (**Supplementary Figure 2B**). CHD-030498 reverted the mesenchymal phenotype at 1 μM, inducing the formation of domed colonies similarly to budesonide (~70%) at 10 μM (**Supplementary Figure 2B**).

These results suggest that CHD-030498 counteracts the acquisition of the mesenchymal phenotype with a higher potency than budesonide and the other analogues.

3.3 EsMT inhibitory activity of BA-GCs is independent of the glucocorticoid receptor (GR)

We recently showed that budesonide inhibitory effect on esMT is independent of the glucocorticoid receptor (GR) [13]. We thus asked whether GR was involved in BA-GC-mediated inhibition of esMT. To address this question, we used *Nuclear Receptor Subfamily 3 Group C Member 1* (*Nr3c1*, GR) knocked down (KD) ESC lines [13]. We first tested the ability of *Nr3c1* KD ESCs to proliferate and eventually to undergo esMT. The analysis of the EdU incorporation showed comparable EdU intensity means in both Control (shNT, not targeting) and sh*Nr3c1* ESC lines in absence of proline (**Supplementary Figure 3A**). Moreover, proline supplementation induced proliferation of both shNT and sh*Nr3c1*#2 ESCs at the same extent, as indicated by increased EdU incorporation (**Supplementary Figure 3A**), thus suggesting that *Nr3c1* KD does not affect ESC proliferation.

We then analysed the effect of *Nr3c1* KD on esMT. The quantification analysis (domed *versus* flat shaped colonies) showed that the fraction of domed colonies was comparable in the sh*Nr3c1 #1-3* cell lines and shNT control cells (**Figure 3A**), thus indicating that *Nr3c1* KD ESCs undergo esMT. These results were further confirmed at molecular level by qPCR expression analysis of the mesenchymal markers *Fgf5*, *N-Cadherin* and *Brachyury/T*. Specifically, we found that expression of all the genes analysed was strongly and similarly induced in both shNT and sh*Nr3c1*#2 ESCs upon proline supplementation (**Supplementary Figure 3B**).

Based on the evidence that a high levels of GR expression is dispensable for esMT, we tested budesonide and BA-GCs on *Nr3c1* KD ESCs during the esMT transition. Thus, control shNT and sh*Nr3c1*#2 cell line were plated at low density (300 cells/cm^2) on gelatin-coated plates and treated ± proline (500 μM), ± budesonide and fluticasone as controls and ± BA-GCs at the active concentrations. As expected, budesonide, but not fluticasone, inhibited proline-dependent acquisition of mesenchymal/flat morphology in sh*Nr3c*1 ESCs as efficiently as in the shNT control (**Figure 3B**). BA-GCs used at 10 μM, with the exception of CHF6162.00, inhibited esMT also in the absence of GR (**Figure 3C**). Of note, in the presence of 1 μM CHD-030498 the sh*Nr3c1*#2 cell lines were unable to undergo esMT.

These findings suggest that CHD-030498 is a potent BA-GC, able to inhibit esMT in a GR-independent manner, remarkably at a concentration 10 times lower than all the other compounds assayed.

 doi:10.20944/preprints202305.2155.v1

3.4 BA-GCs counteracts exit from pluripotency in cell colonies and spheroids

We next tested the effect of the most potent BA-GC, *i.e.* CHD-030498, on spontaneous ESC differentiation induced by 2i/LIF withdrawal. Thus, ESCs were first cultured in FBS/2i/LIF for 3 days and then shifted to a medium containing FBS ± CHD-030498 or budesonide or kept in FBS/2i/LIF as controls. After further 4 days in culture the colony morphology was analysed (**Figure 4A**). As previously described [13], while FBS/2i/LIF and budesonide-treated ESC colonies maintained a domed-shaped and regular morphology, untreated cell colonies undergo a morphological transition, generating flat-irregular colonies (96,6%±2,4) (**Figure 4A and B**). Differently from budesonide, fluticasone and CHD-032201 were unable to counteract spontaneous differentiation (Supplementary **Figure 4A, data not shown**). Similarly to budesonide, CHD-030498-treated ESC colonies maintained the domed-shaped morphology in a dose-dependent manner. Indeed, the generation of differentiated flat-shaped cell colonies was reduced from 84.4±1.8, to 64.4±13.6, and 35.9±5.6 % at 1, 2.5, and 5 μM CHD-030498, respectively (**Figure 4B**). At 10 μM CHD-030498 only small colonies were formed (**Figure 4B**), consistently with the observed reduction of ESC proliferation and induction of apoptosis at this concentration (see **Figure 1**). Our results suggest that CHD-030498 is able to counteract exit from pluripotency induced by removal of 2i/LIF by promoting the generation of highly compacted cell colonies, and inducing the stabilization of cell-cell interactions.

We finally assessed the ability of CHD-030498 to counteract spontaneous differentiation also in 3D culture conditions (**Figure 4C**). To this aim naïve pluripotent ESCs were seeded by FACS in ultra-low attachment U-round bottom plates (300 cells/well, 96-well plate) and allowed to aggregate in N2B27 medium supplemented with 2i/LIF for 24 hrs, to generate highly compacted floating spheroids. The spheroids were then shifted to different conditions including DMSO alone (differentiating conditions), 2i/LIF (pluripotency maintenance), budesonide (10 μM) or CHD-030498 used at different concentration from 1 μM and 10 μM (**Figure 4C and Supplementary Figure 4C**). Similarly to budesonide, CHD-030498-treated ESC spheroids maintained a domed-shaped morphology and a reduced dimension, in a dose dependent manner. Moreover, the resulting spheroids (8-day-old) were highly compacted and similar to 2i plus LIF condition, as shown by E-cadherin staining (**Figure 4D**). By contrast, in the absence of inhibitors/cytokines (2i/LIF), untreated spheroids (DMSO) showed an irregular/loose structure, suggesting a differentiation process (**Figure 4D**). Our results suggest that CHD-030498 is able to counteract exit from pluripotency in 3D spheroids, induced by removal of 2i/LIF.

3.5 BA-GCs prevent symmetry breaking and gastruloid elongation

We then evaluated the effect of CHD-030498 on gastruloid development. To this end, ESCs cultured in naïve pluripotency-inducing conditions (2i/LIF) were FACS-sorted in ultra-low attachment U-round bottom plates (300 cells/well); budesonide, CHD-032201 and CHD-030498, were added at 1 μM and 10 μM within the 0-48 hour-time window (**Figure 5A**). At day 2 and 5 the resulting organoids were imaged, the diameter was measured and the elongation index (EI) was calculated. As previously shown, 10 μM budesonide reduced the diameter of 2-day-old aggregates compared to control [13]. At day 5, control aggregates efficiently elongated, whereas budesonide-treated aggregates failed to develop into fully elongated gastruloids (EI=~1,5-2) (**Figure 5B**)[13]. Indeed, 10 μM CHD-032201 allowed the generation of small-sized spheroids, which maintained a spheroidal shape even after 5 days of incubation (**Figure 5B**). Finally, CHD-030498 and CHD-032201 at 10 μM showed toxic effects at both day 2 and 5 (**Figure 5B**).

Since the formation of spheroids with a precise diameter (around 150-180 μm) is an essential step for the proper development of elongated gastruloids [18], we analysed the effect of a lower concentration (1 μM) of BA-GCs on ESCs aggregation. Similarly to 1 μM Budesonide, ESCs treated with 1 μM CHD-032201 were able to form properly shaped and sized aggregates, which eventually elongated in 3D gastruloids (**Figure 5C**). By contrast,

Preprints (www.preprints.org) | NOT PEER-REVIEWED | Posted: 30 May 2023 doi:10.20944/preprints202305.2155.v1

1 μM CHD-030498 induced the generation of small aggregates, which failed to elongate, showing an effect similar to that of 10 μM budesonide (**Figure 5B and 5C**). Moreover, CHD-030498- treated aggregates (1 μM) did not express the developmental markers Brachyury (Bra, T) and Cdx2, and stained positive for the pluripotency markers Oct4 and Nanog, similar to that observed with budesonide (10 μM) (**Figure 5D**). We next performed a dose-dependent (ranging from 1 to 0.1 μM) gastruloid formation assay in the presence of CHD-030498 throughout the experiment (0-120 hrs) (**Supplementary Figure 5**). Indeed, the EI significantly decreased when the concentration of CHD-030498 increased reaching a value of 2.7, 1.9, 1.3, and 1, at 0.125, 0.25, 0.5 and 1 μM, respectively (**Figure 5E and Supplementary Figure 5C**). At 0.125 μM CHD-030498 the EI was comparable to control (**Supplementary Figure 5C**) and, accordingly, the elongated gastruloids correctly expressed Bra (**Supplementary Figure 5D**).

In conclusion, our results suggest that only CHD-030498 affects gastruloid development acting similarly to budesonide, but at a lower concentration.

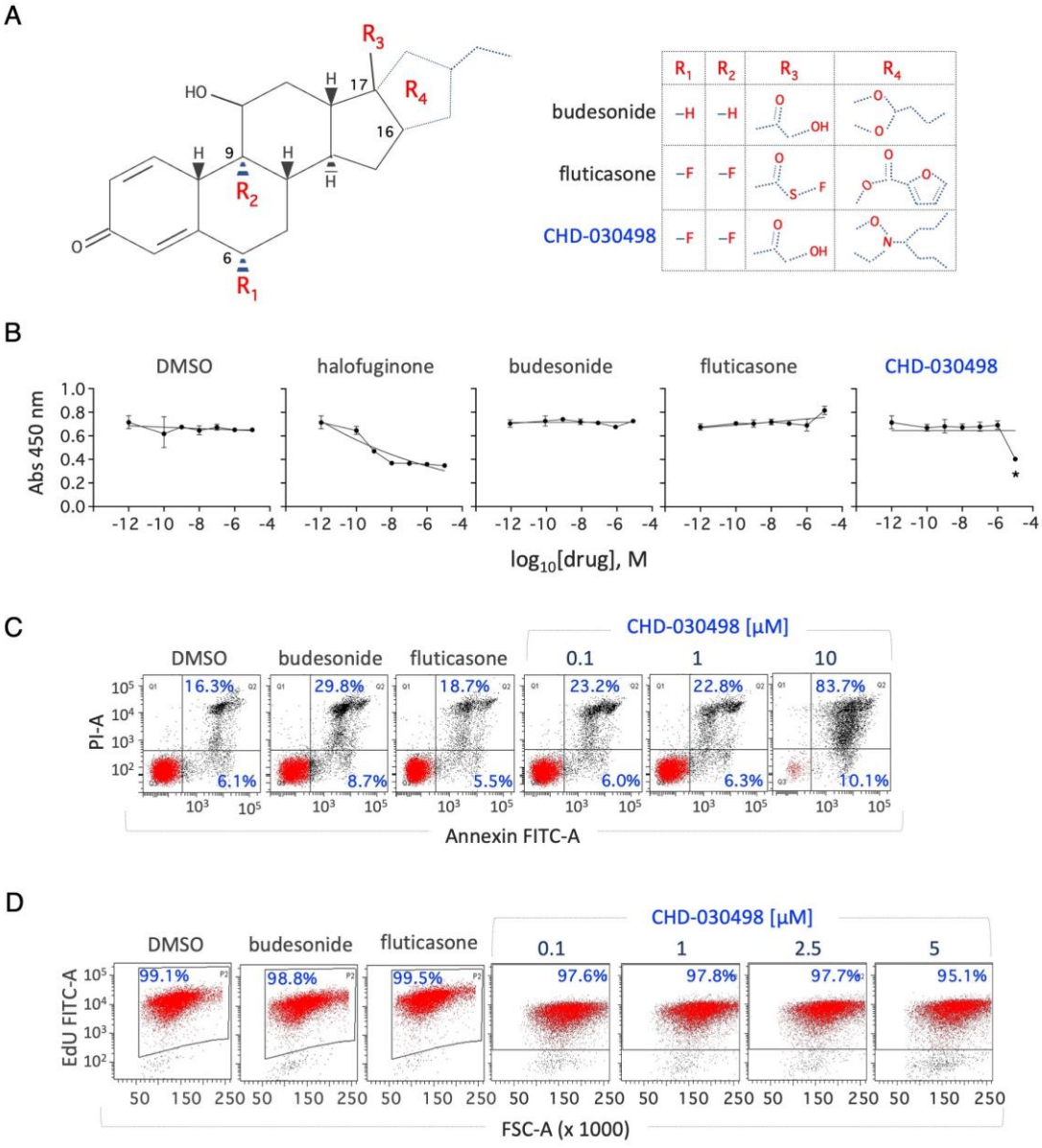

Figure 1. Effect of CHD-030498 on ESCs proliferation. (A) Basic 4-ring steroid backbone of glucocorticoids is shown. Residual groups (from R1 to R4) for budesonide, fluticasone and CHD-030498 are represented. (B) Cell survival was analyzed using the CCK-8 cytotoxicity assay, after 48 hrs of

 doi:10.20944/preprints202305.2155.v1

treatment. Compounds were tested in a large concentration range (from 10^{-10} to 10^{-5} M). Halofuginone was used as a positive (toxic compound) Control. Data are shown as mean ± SD (n=3; *p≤0.01). (C) FACS analysis of apoptotic cells. Representative dot plot of Annexin V/PI staining in ESCs treated with DMSO, budesonide (10 µM), fluticasone (10 µM) and CHD-030498 (0.1, 1 and 10 µM). The fraction (%) of Annexin V+ (bottom right) and Annexin V+/ PI+ (up) cells are indicated. Annexin V is conjugated with FITC. (D) Dose-response effect of CHD-030498 on ESC proliferation. Representative dot plot of EdU incorporation in ESCs treated with DMSO, budesonide (10 ◎M), fluticasone (10 µM) and CHD-030498 (0.1, 1, 2.5 and 5µM). The fraction (%) of cells that incorporated EdU is shown.

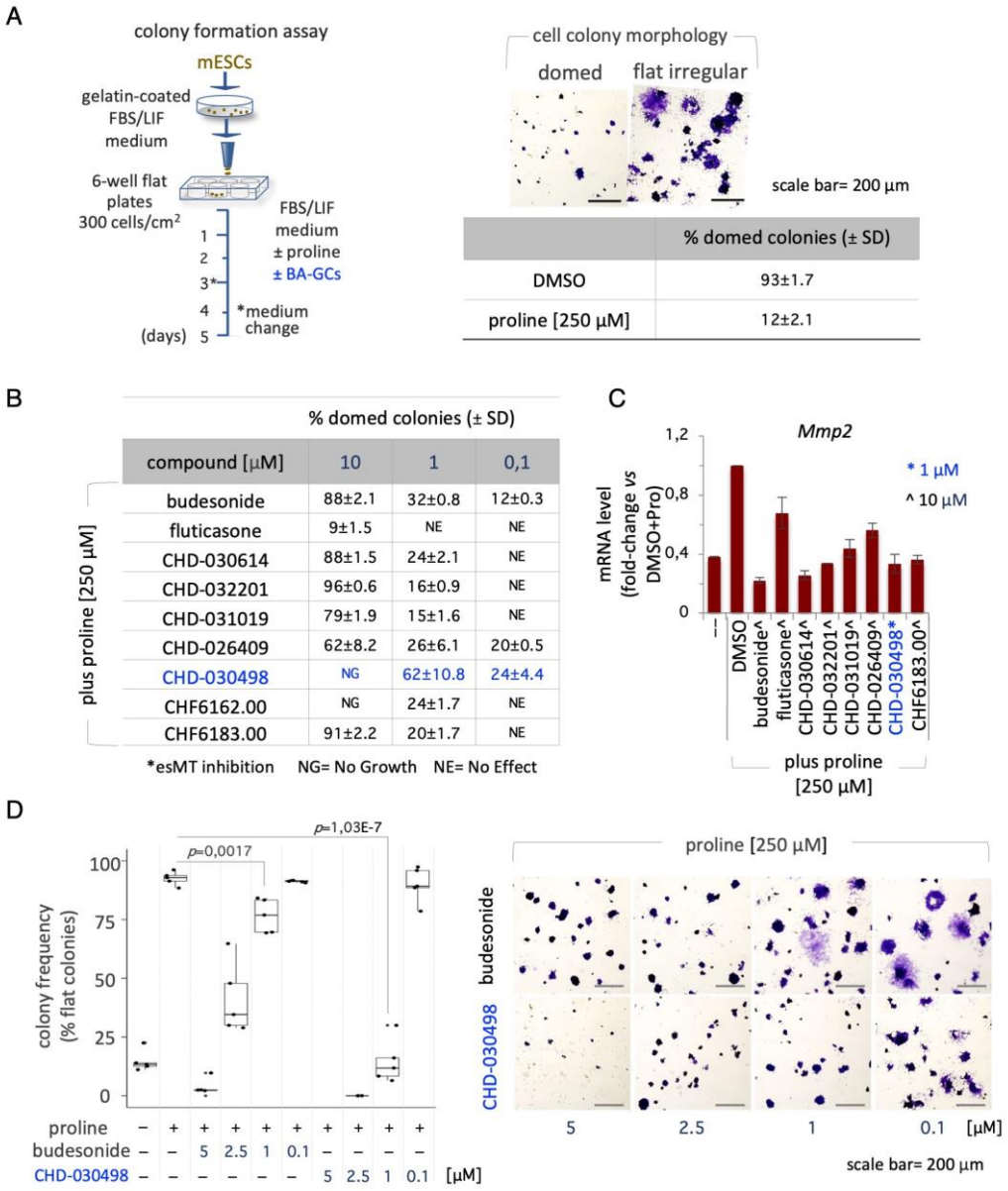

Figure 2. Effect of BA-GCs on embryonic stem cell-to-mesenchymal transition (esMT). (A) Schematic representation of the experimental procedure (left). Representative photomicrographs of domed/regular- and flat/irregular-shaped cell colonies (top right) and quantification of the fraction (%) of domed colonies generated from ESCs treated ± proline (250 µM) (bottom right). (B) Table showing the fraction (%) of domed colonies (esMT inhibition) generated from ESCs treated + proline (250 µM) ± BA-GCs supplemented at the indicated concentrations. Budesonide and fluticasone were used, respectively, as a positive (esMT inhibitor) and negative (inactive) Control. Data are shown as mean ± SD (n=3). (C) Effect of BA-GCs on the expression of matrix metallopeptidase 2 (*Mmp2*) gene. qPCR analysis was performed using total RNA extracted after 48 hrs of treatment with proline (250

Preprints (www.preprints.org) | NOT PEER-REVIEWED | Posted: 30 May 2023 doi:10.20944/preprints202305.2155.v1

μM) ± BA-GCs (10 μM). CHD-030498 was used at 1 μM. Values are expressed as fold-change *versus* DMSO-treated ESCs, after normalization to *Gapdh* and are mean ± SEM (n=3). (D) Dose-dependent effect of CHD-030498 on esMT. Representative photomicrographs (right) and quantification (left) of the colonies generated from ESCs treated ± proline (250 μM), plus CHD-030498 at 0.1, 1, 2.5 and 5 μM. Data are shown as mean ± SD (n=3).

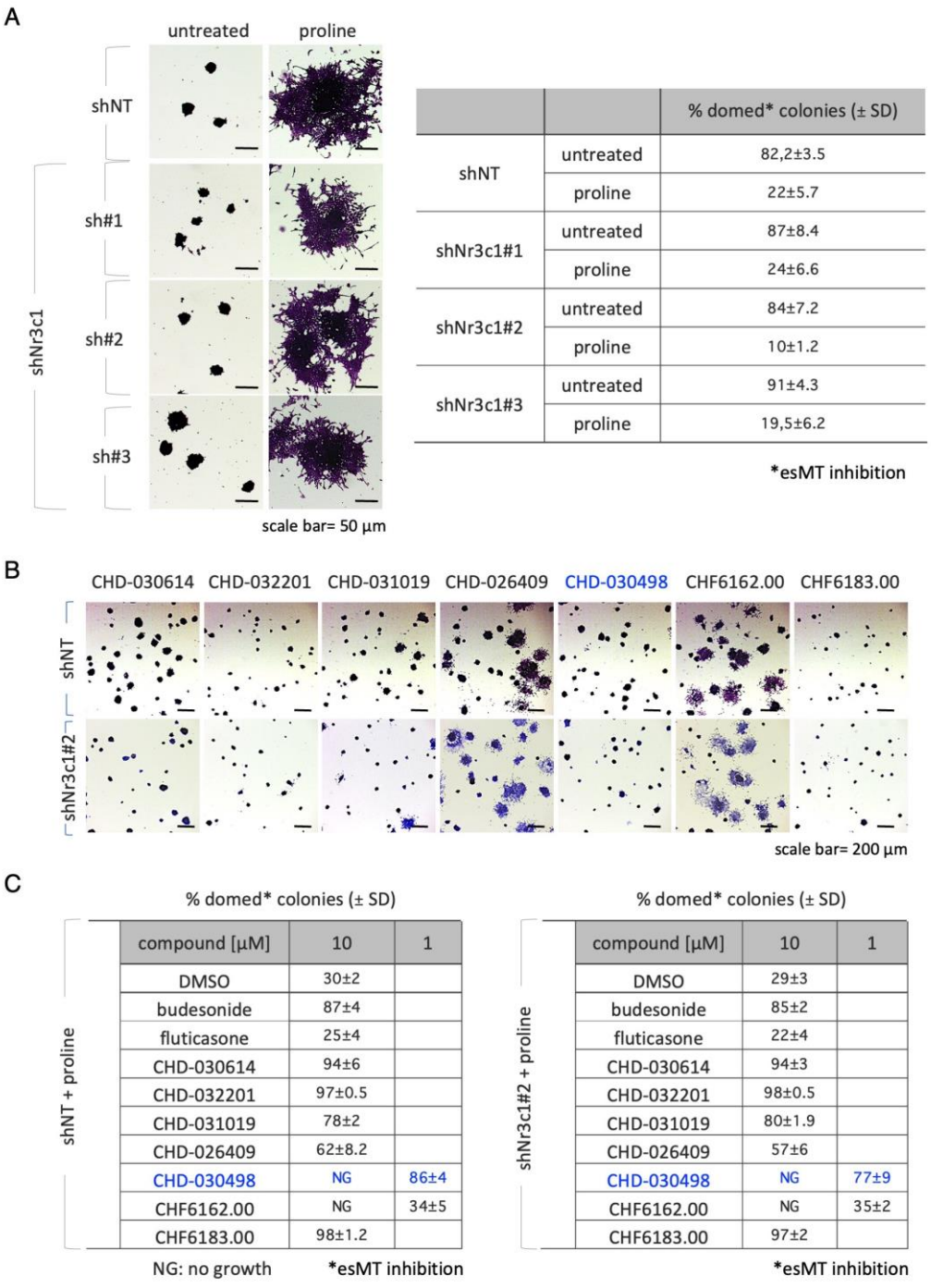

		% domed* colonies (± SD)
shNT	untreated	82,2±3.5
	proline	22±5.7
shNr3c1#1	untreated	87±8.4
	proline	24±6.6
shNr3c1#2	untreated	84±7.2
	proline	10±1.2
shNr3c1#3	untreated	91±4.3
	proline	19,5±6.2

*esMT inhibition

Figure 3. Effect of Glucocorticoid receptor on BA-GCs-mediated modulation of esMT. (A) Representative photomicrographs (left) of cell colonies generated from shNT (non-targeting Control) and shNr3c1#2 (GR knock-down) ESCs under esMT-inducing condition (supplemental proline, 500 μM). Table showing the fraction (%) of domed-shaped cell colonies (esMT inhibition) (right). Scale bar, 50 μm. (B) Representative photomicrographs of colonies generated from shNT and shNr3c1#2 ESCs treated ± proline (500 μM) ± BA-GCs (10 μM), and stained with Crystal violet. CHD-030498 was used at 1 μM. (C) Tables showing the fraction (%) of domed colonies (esMT inhibition), in the

Preprints (www.preprints.org) | NOT PEER-REVIEWED | Posted: 30 May 2023 doi:10.20944/preprints202305.2155.v1

different conditions (shNT, bottom left; sh*Nr3c1*#2, bottom right). Budesonide and fluticasone were used as a positive (esMT inhibitor) and negative (inactive) Controls. Data are shown as mean ± SD (n=3). Scale bar, 200 μm.

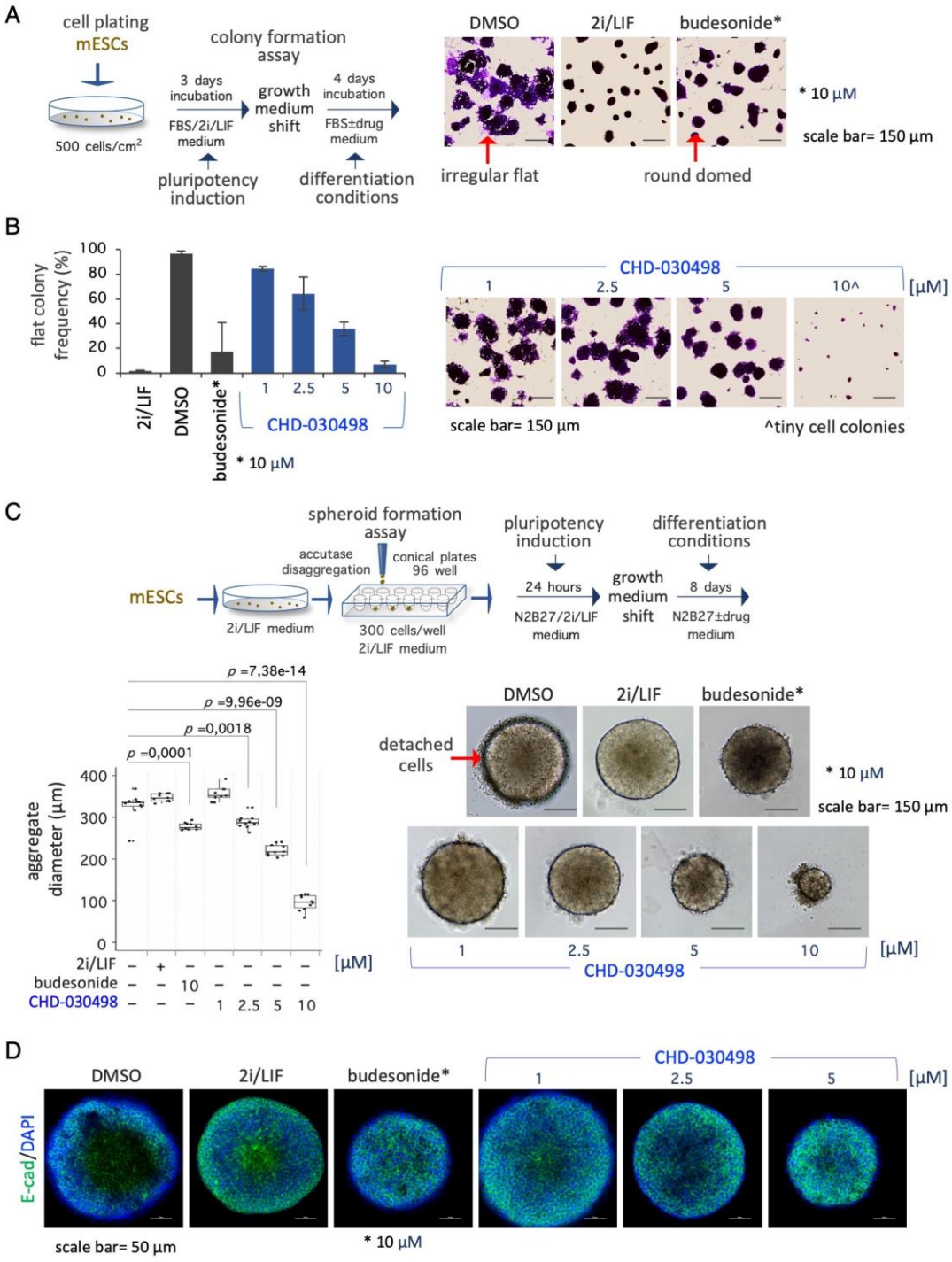

Figure 4. Effect of BA-GCs on pluripotency exit. (A) Schematic representation of the experimental procedure (left). ESCs were plated (500 cells/cm²) in DMEM/FBS/2i/LIF medium for 3 days. The resulting domed-shaped colonies were shifted to DMEM/FBS medium supplemented with DMSO, 2i/LIF, fluticasone, or budesonide. After 4 days of incubation the cell colonies were imaged or fixed and stained with crystal-violet (right). Scale bar, 150 μm. In the absence of undifferentiating factors, such as the 2i/LIF mix, ESCs proliferate generating irregular flat- instead of round domed-shaped

Preprints (www.preprints.org) | NOT PEER-REVIEWED | Posted: 30 May 2023 doi:10.20944/preprints202305.2155.v1

cell colonies. (B) Dose-response activity of CHD-030498 on the morphological transition associated with pluripotency exit. Histogram showing the fraction (%) of flat-shaped cell colonies (left) generated in the presence of budesonide (10 μM, used as a positive control), or CHD-030498 (from 1 to 10 μM). Data are mean ± SD (n = 3; 10 fields/condition). Representative images of crystal violet-stained cell colonies (right). Scale bar, 150 μm. (C) Schematic representation of the experimental procedure (top). Pluripotent ESCs (2i/LIF) were FACS sorted (300 cells/well) on 96-well ultra-low conical plates and incubated in N2B27 ± CHD-030498 (from 1 to 10 μM). After 7 days of incubation the resulting spheroids were imaged and measured. Boxplot diagrams of aggregate diameter at day 7 (left; 10 spheroids/condition), and representative bright-field images (right) of spheroids treated with DMSO (control), or CHD-030498 used at the indicated concentration. Scale bar, 150 μm. (D) Immunofluorescence analysis of E-cadherin (E-cad) expression. Representative confocal images of 8-day-old spheroids, generated as described in (C). Nuclei were counterstained with DAPI (blue). Scale bar, 50 μm.

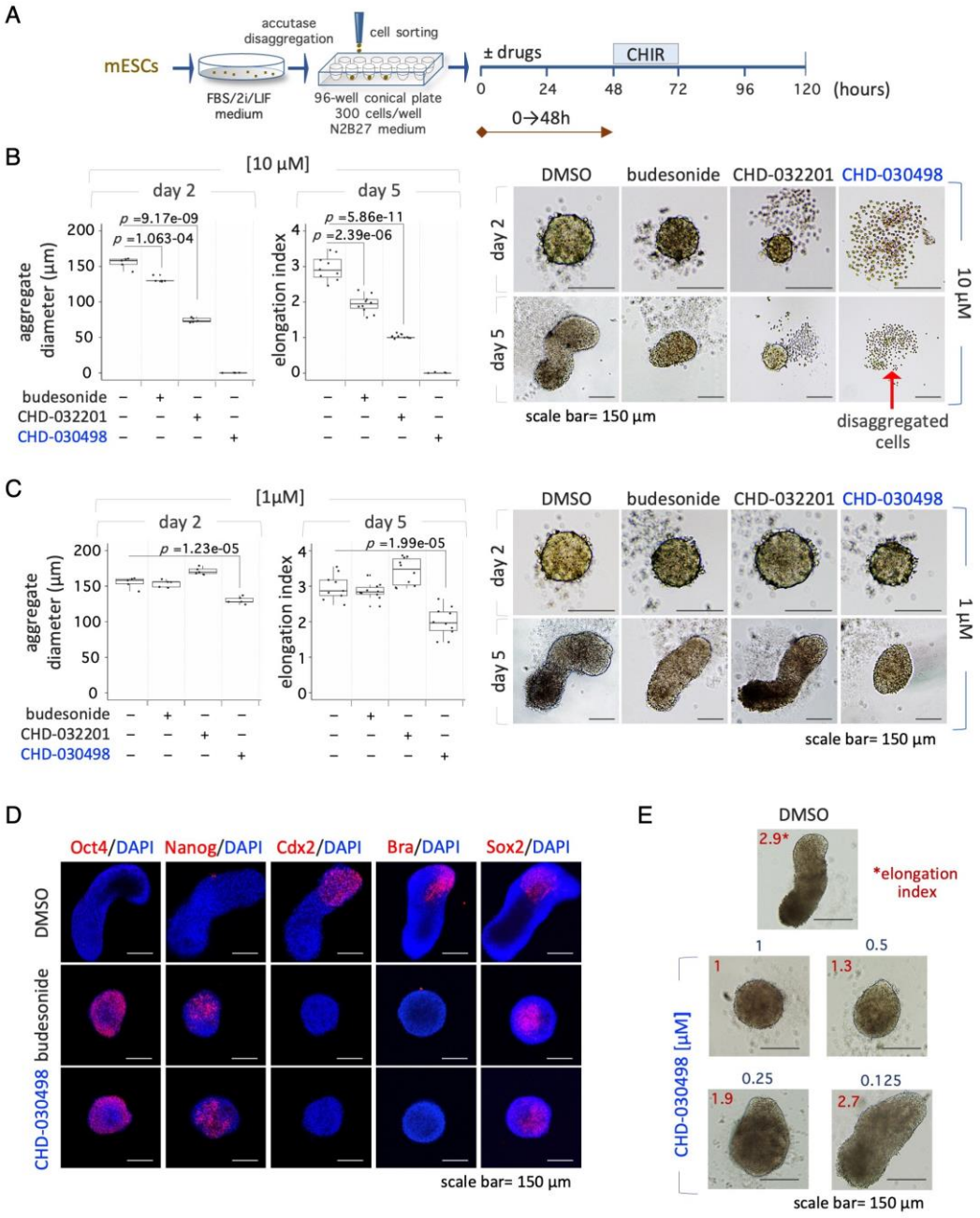

Figure 5. Effect of BA-GCs on gastruloid development. (A) Schematic representation of the experimental design. Pluripotent ESCs (2i/LIF) were FACS sorted (300 cells/well) on 96-well ultra-low

Preprints (www.preprints.org) | NOT PEER-REVIEWED | Posted: 30 May 2023 doi:10.20944/preprints202305.2155.v1

conical plates and incubated in N2B27 ± CHD-032201 or CHD-030498 (10 and 1 μM). (B-C) Boxplot diagrams of aggregate diameter at day 2 (left; 10 aggregates/condition), and of gastruloid elongation index (middle) and representative bright-field images (right) of gastruloids treated with DMSO (control), CHD-032201, or CHD-030498 at 10 (B) and 1 μM (C) (10 gastruloids/condition). Scale bar, 150 μm. (D) Immunofluorescence analysis of pluripotency (Oct4, Nanog) and differentiation (Cdx2, Brachyury, Sox2) marker expression. Representative confocal images of 5-day-old aggregates/gastruloids, untreated or treated with budesonide (10 μM, positive control) or with CHD-030498 (1 μM). Nuclei were counterstained with DAPI (blue). Scale bar, 150 μm. (E) Dose-dependent effect of CHD-030498, added at 1, 0.5, 0.25 and 0.125 μM, from T0 to 120 hrs. The elongation index is shown (10 gastruloids/condition). Scale bar, 150 μm.

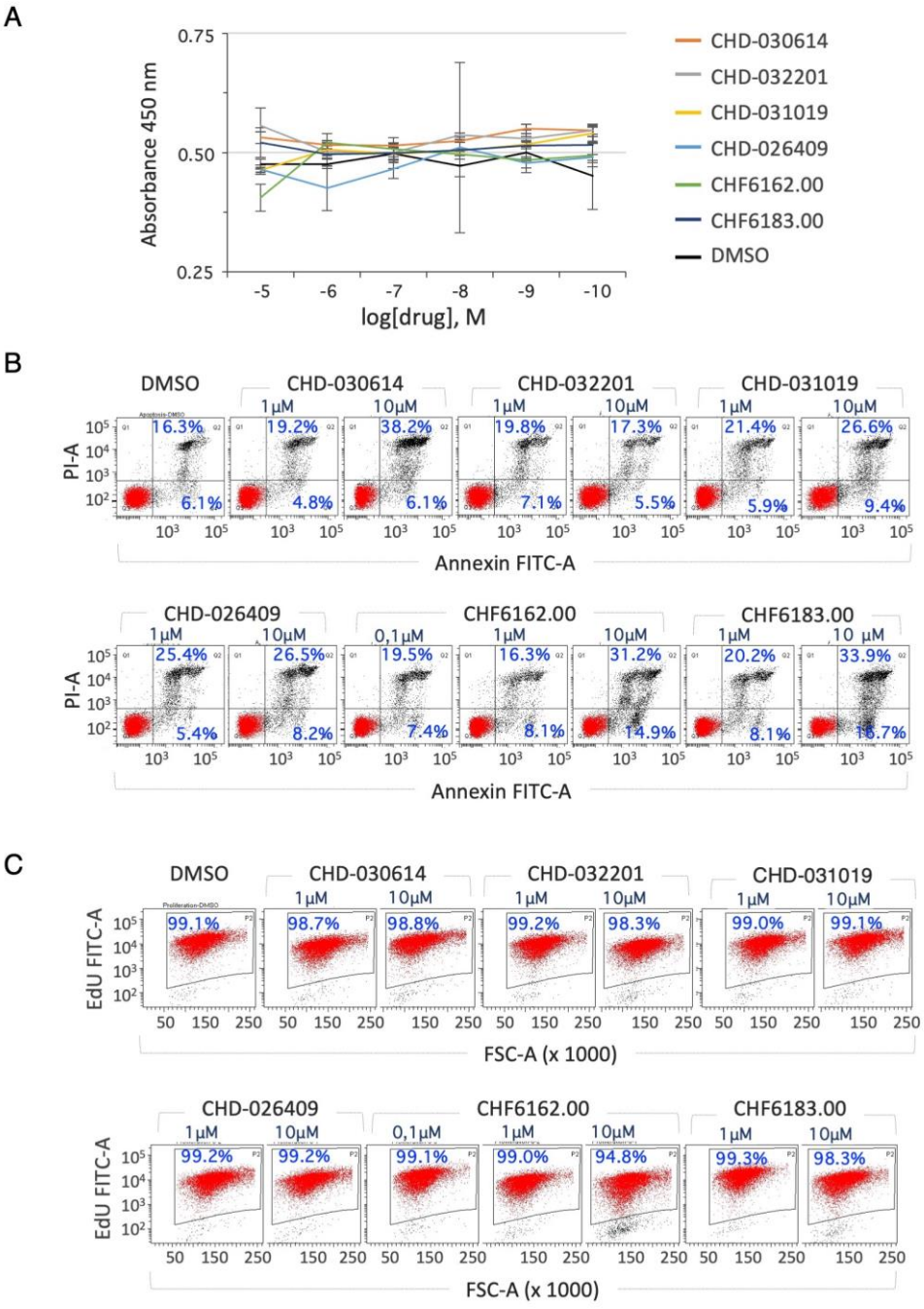

Supplementary Figure 1. Effect of BA-GCs on ESCs proliferation. (A) Effect of BA-GCs on ESC survival at the following concentrations: 10^{-10}, 10^{-9}, 10^{-8}, 10^{-7}, 10^{-6}, 10^{-5} M, for 48 hrs, by CCK-8 assay. Data are shown as mean ± SD (n=3; *p≤0,01). (B) FACS analysis of apoptotic cells. Representative

Preprints (www.preprints.org) | NOT PEER-REVIEWED | Posted: 30 May 2023 doi:10.20944/preprints202305.2155.v1

dot plot of Annexin V/PI staining in ESCs treated with DMSO as Control, and treated with the different BA-GCs used at the indicated concentrations. The fraction (%) of Annexin V+ (bottom right) and Annexin V+/ PI+ (top right) cells are shown. Annexin V is conjugated with FITC. (C) FACS analysis of EdU incorporation. Representative dot plot of EdU incorporation in ESCs treated with DMSO as Control, and treated with BA-GCs at the indicated concentrations. The fraction (%) of cells that incorporated EdU is shown.

A

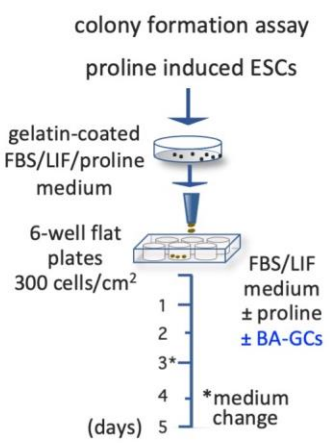

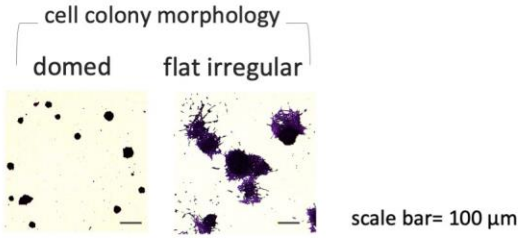

	% domed colonies (± SD)
DMSO	67±2
proline	33±1.7

B

% domed* colonies (± SD)

	compound [µM]	10	1
proline plus	budesonide	74±0.9	40±1.2
	fluticasone	36±1.6	NE
	CHD-030614	79±1.9	54±2
	CHD-032201	89±1.2	35±0.9
	CHD-031019	52±0.7	40±1.3
	CHD-026409	40±2.3	40±1.8
	CHD-030498	NG	70±3
	CHF6162.00	NG	40±1.6
	CHF6183.00	67±0.8	45±0.7

*MesT induction NG= No Growth NE= No Effect

Supplementary Figure 2. Effect of BA-GCs on mesenchymal-to-embryonic stem cell transition (MesT). (A) Schematic representation of the experimental procedure (left). Representative photomicrographs of domed- and flat-shaped cell colonies (top right) and quantification of the fraction (%) of domed-shaped cell colonies generated from proline-induced mesenchymal-like cells treated ± proline (250 µM) (bottom right). (B) Table showing the fraction (%) of domed-shaped cell colonies (MesT induction), generated from proline-induced mesenchymal-like cells treated with proline (250 µM) ± BA-GCs at the indicated concentrations. Budesonide and fluticasone were used as a positive (MesT inducer) and negative (inactive) Control. Data are shown as mean ± SD (n=3).

 doi:10.20944/preprints202305.2155.v1

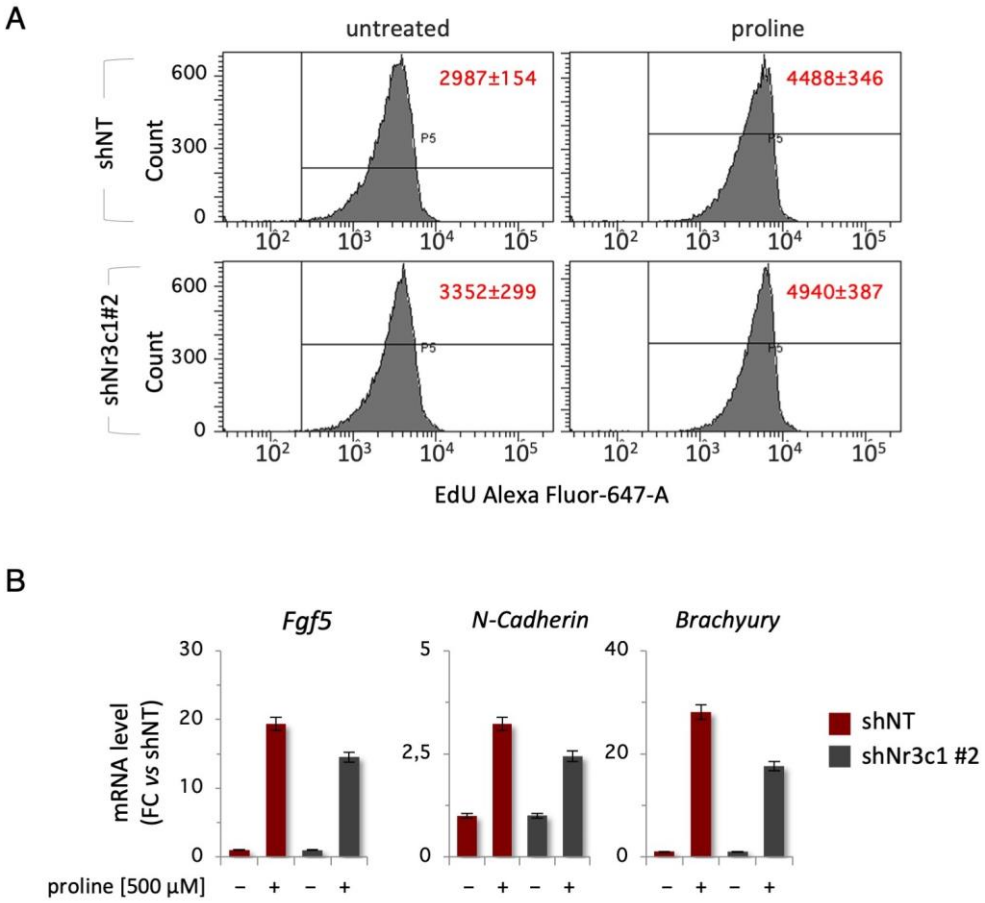

Supplementary Figure 3. Effects of proline on the proliferation of GR knock-down cells. (A) FACS analysis of proliferating cells. Representative histograms of EdU incorporation in shNT and shNr3c1#2 ESCs ± proline (500 µM) are shown. The mean intensity of EdU incorporation is shown. Data are mean ± SEM (n=3). (B) Effect of GR on the expression of esMT marker genes. qPCR analysis of *Fibroblast Growth Factor 5* (*Fgf5*), *Neural Cadherin* (*N-Cadherin*) and *Brachyury* gene expression. Values are expressed as a fold-change *versus* shNT ESCs, after normalization to *Gapdh* and are mean ± SEM (n=3).

Preprints (www.preprints.org) | NOT PEER-REVIEWED | Posted: 30 May 2023 doi:10.20944/preprints202305.2155.v1

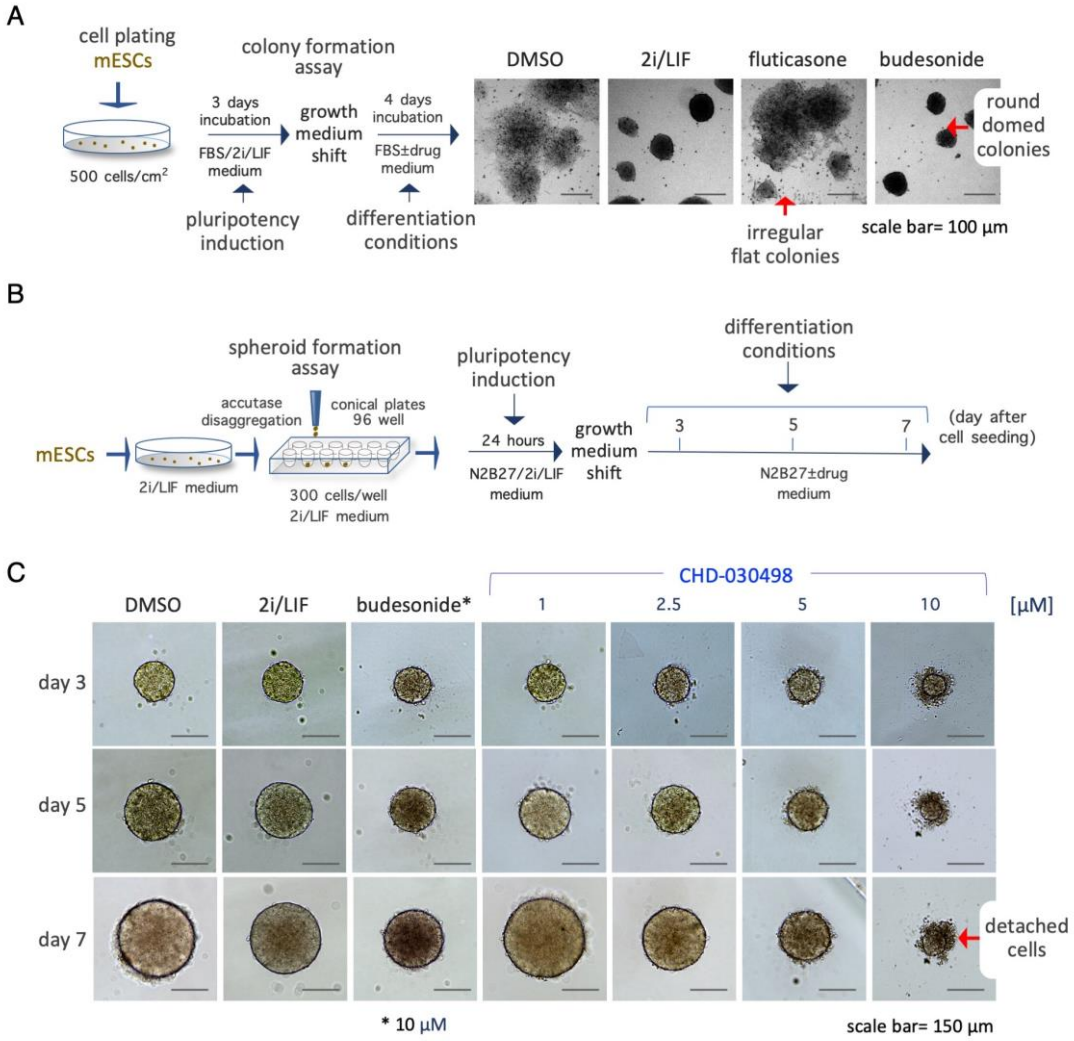

Supplementary Figure 4. Time-course and dose-response effect of CHD-030498 on pluripotency-exit. (A) Schematic representation of the pluripotency exit procedure (left). ESCs were plated (500 cells/cm²) in DMEM/FBS/2i/LIF medium for 3 days, and then shifted to DMEM/FBS medium supplemented with DMSO, 2i/LIF, fluticasone, or budesonide. After 4 days of incubation the cell colonies were imaged (bright-field images; right). Scale bar, 100 µm. (B) Schematic representation of the experimental procedure. ESCs (2i/LIF) were FACS sorted (300 cells/well) on 96-well ultra-low conical plates and incubated in N2B27 ± DMSO, 2i+LIF or CHD-030498 (from 1 to 10 µM). (C) Representative bright-field images of spheroids obtained as described in (B). Images were captured for each condition at day 3, 5 and 7. and measured. Scale bar, 150 µm.

Preprints (www.preprints.org) | NOT PEER-REVIEWED | Posted: 30 May 2023 doi:10.20944/preprints202305.2155.v1

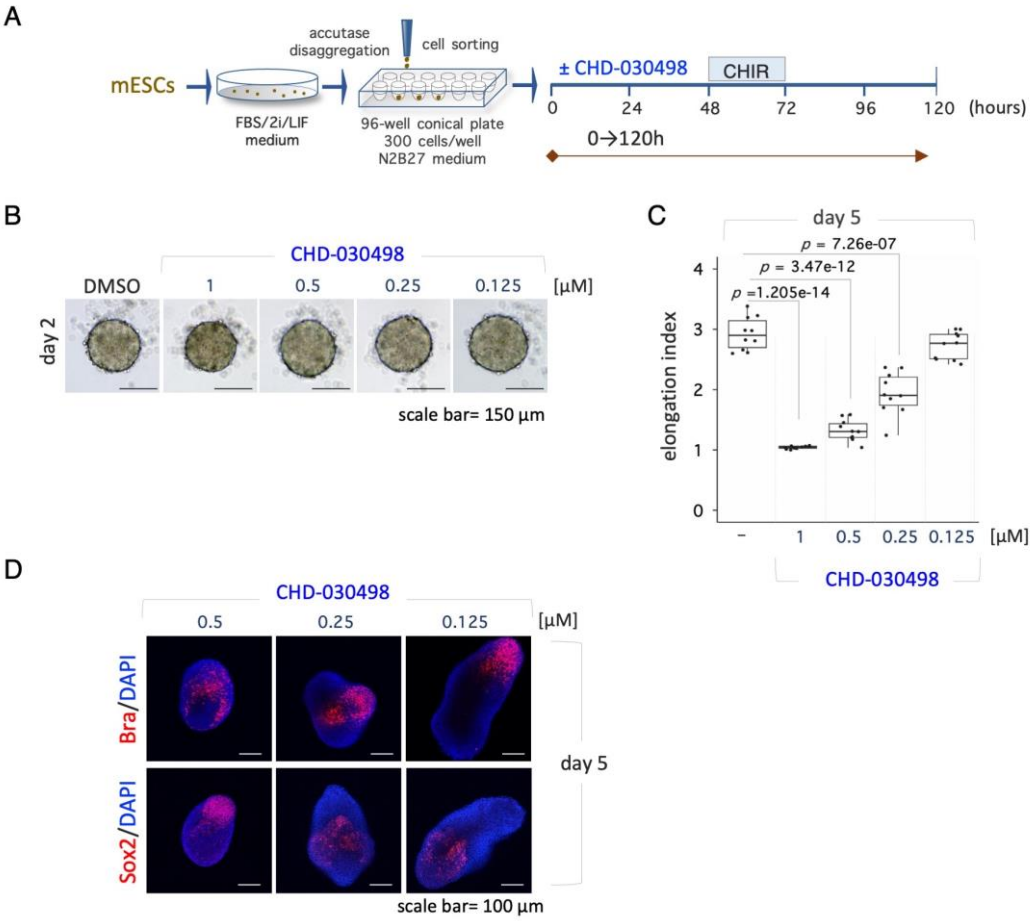

Supplementary Figure 5. Dose-response activity of CHD-030498 on gastruloid development. (A) Schematic representation of the experimental design. Naïve pluripotent (2i/LIF) ESCs were FACS sorted (300 cells/well) on 96-well ultra-low conical plates in N2B27 ± CHD-030498 added at 1, 0.5, 0.25 and 0.125 μM, from t0 to t120 hrs. (B) Boxplot diagrams of gastruloid elongation index (left) and representative bright-field images (right) of 2-day-old aggregates treated with DMSO (control), or CHD-030498 at 1, 0.5, 0.25 and 0.125 μM (n = 3; 20 gastruloids/condition). Scale bar, 150 μm. (C) Immunofluorescence analysis of differentiation (Brachyury, Sox2) markers. Representative confocal images of 5-day-old aggregates/gastruloids treated with CHD-030498 added at the indicated concentrations. Nuclei were counterstained with DAPI (blue). Scale bar, 100 μm.

4. Discussion

In this study we have analysed the effects of a small set of synthetic glucocorticoids (budesonide analogues glucocorticoids; BA-GCs), using 2D and 3D stem cell-based assays, as an *in vitro* paradigm of pluripotency exit.

Over the last years, the use of small molecules has largely increased, as a complementary approach to the classical genetics, to investigate several biological functions. In particular, small molecules have represented useful tools to study stem cell biology and explore the underlying mechanisms of stem cell self-organization and cell-cell communication, by which initially homogeneous populations of cells break symmetry and undergo *in vivo*-like pattern formation and morphogenesis. These mechanisms are attracting great interest in the emerging field of synthetic embryology, and are still poorly defined.

Here we compared the activity of the BA-GCs on ESCs to that recently described for budesonide [13]. Our results indicate that most of the BA-GCs counteract exit from pluripotency on different *in vitro* models, including spontaneous differentiation (LIF/2i withdrawal) and esMT triggered by proline supplementation, at levels comparable to that of

 doi:10.20944/preprints202305.2155.v1

budesonide. Interestingly, among the BA-GCs, one compound, named CHD-030498 show increased activity, being able to inhibit the naïve to primed transition induced by proline at a concentration ten times lower than budesonide. The morphological changes are associated to variations at a molecular level. Indeed, *Mmp-2*, a gene induced by proline, is inhibited by the BA-GCs. In particular, CHD-030498 reduces *Mmp-2* levels similarly to budesonide, but at a lower concentration. CHD-030498 also promoted the reversed transition, facilitating the formation of pluripotent/domed colonies in the presence of proline, and showing a higher efficacy than budesonide and the other BA-GCs, acting at 1 μM. Of note, while none of the tested compounds shows a toxic effect on ESCs, only CHD-030498 reduces ESC survival and induces apoptosis at the higher concentration. However, when reducing its concentration (from 5 to 1 μM), proliferation is not altered anymore.

Budesonide has been recently shown to inhibit exit from pluripotency in 2D ESC cultures in a glucocorticoid-independent manner [13]. Our findings show that BA-GCs ability to counteract pluripotency exit is independent from the GR, suggesting that similarly to what observed for budesonide other targets may be involved. In support of our conclusions, fluticasone and the *Nr3c1* knock down do not affect pluripotency exit, as previously shown [13].

Budesonide has been shown to inhibit exit from pluripotency also in 3D gastruloids, promoting cell-cell adhesion and compaction. Similarly, CHD-030498 keeps round and compacted floating aggregates and avoids pluripotency exit and gastruloid development. Of note, as for 2D cultures, CHD-030498 inhibits pluripotency exit in 3D gastruloids at a concentration ten times lower compared to budesonide. Interestingly, another BA-GC, namely CHD-032201, is active in 2D cultures, but not on 3D cell aggregates, highlighting the differences between 2D and 3D cultures and the importance of comparing drug effects in both conditions.

CHD-030498-dependent inhibition of pluripotency exit is supported by the persistent expression of the pluripotency markers Oct4 and Nanog in 3D gastruloids/aggregates and the absence of the differentiation markers Cdx2 and Bra. Of note, also CHD-030498-dependent molecular effects occur at a concentration ten times lower than budesonide. The molecular mechanisms underlying the establishment of stem cellular identity and behaviour during development are still largely unknown. However, the study of the molecular effects of BA-GCs, such as CHD-030498 might be helpful to elucidate how cell-cell interactions influence pluripotency exit and differentiation.

Budesonide belongs to the corticosteroid class of medications, commonly used to treat inflammatory diseases, including asthma, Crohn disease and ulcerative colitis. In spite of their beneficial effects, collateral unwanted reactions are often observed following high doses and prolonged corticosteroid treatment. These adverse effects have been mainly ascribed to GR independent 'nongenomic' effects, which hinge on nonspecific interactions of steroidal molecules with cellular membranes.

In light of these considerations, the identification of a novel budesonide analogue, *i.e.*, CHD-030498, which shows effects similar to budesonide but at a significant lower concentration, may help to develop a potentially less toxic drug for other applications.

Budesonide has been shown to reduce extracellular collagen accumulation (fibrosis), stabilize the cell-cell interactions in primary tumors, and decrease the appearance of lung metastasis in orthotopic breast cancer xenograft [14]. Thus, it would be interesting in the future to assess the effect of CHD-030498 in pathological contexts, including cancer progression and fibrotic diseases.

In conclusion, our findings highlight CHD-030498 as a potent inhibitor of cellular plasticity both on 2D systems and on the processes that are dependent on the initial formation of 3D cell aggregates, as gastruloids, acting in a lower concentration range. Changing the budesonide chemical structure has allowed to identify a new bioactive compound with higher potency that would represent a potential novel drug candidate for the treatment of a broad spectrum of diseases in which cell fate transition and fibrosis are involved, including metastatic cancer.

Author Contributions: Conceptualization, G.M., E.J.P., D.D.C. and C.D.; investigation, F.A., E.I, F.S., F.C., G.P. and C.D.; formal analysis, F.A. and E.I.; writing—original draft preparation, D.D.C. and C.D.; writing—review and editing, E.S., F.R., G.V., G.C., G.M., E.J.P., D.D.C. and C.D.; supervision, G.V., G.M., E.J.P., D.D.C. and C.D.; funding acquisition, G.M. and C.D. All authors have read and agreed to the published version of the manuscript."

Funding: This research was funded by Chiesi Farmaceutici S.p.A. to C.D.

Informed Consent Statement: Not applicable.

Acknowledgments: We are grateful to Salvatore Arbucci and members of the Integrated Microscopy and FACS Facilities of IGB-ABT, CNR. We thank Gennaro Andolfi for excellent technical assistance.

Conflicts of Interest: E.S., F.R. and G.V. are employees of Chiesi Farmaceutici S.p.A.

References

1. Gonzalez, A.C., et al., Wound healing - A literature review. An Bras Dermatol, 2016. 91(5): p. 614-620.
2. Rodrigues, M., et al., Wound Healing: A Cellular Perspective. Physiol Rev, 2019. 99(1): p. 665-706.
3. Lei, T., et al., Biomimetic strategies for tendon/ligament-to-bone interface regeneration. Bioact Mater, 2021. 6(8): p. 2491-2510.
4. Yu, Y., et al., Functional Hydrogels and Their Applications in Craniomaxillofacial Bone Regeneration. Pharmaceutics, 2022. 15(1).
5. Duda, G.N., et al., The decisive early phase of bone regeneration. Nat Rev Rheumatol, 2023. 19(2): p. 78-95.
6. Iavarone, F., et al., Cripto shapes macrophage plasticity and restricts EndMT in injured and diseased skeletal muscle. EMBO Rep, 2020. 21(4): p. e49075.
7. Guardiola, O., et al., Induction of Acute Skeletal Muscle Regeneration by Cardiotoxin Injection. J Vis Exp, 2017(119).
8. Prezioso, C., et al., Conditional Cripto overexpression in satellite cells promotes myogenic commitment and enhances early regeneration. Front Cell Dev Biol, 2015. 3: p. 31.
9. Martins-Lima, C., et al., Tumor microenvironment and epithelial-mesenchymal transition in bladder cancer: Cytokines in the game? Front Mol Biosci, 2022. 9: p. 1070383.
10. Zhang, J., et al., Regulation of epithelial-mesenchymal transition by tumor microenvironmental signals and its implication in cancer therapeutics. Semin Cancer Biol, 2023. 88: p. 46-66.
11. Yu, L., et al., Blastocyst-like structures generated from human pluripotent stem cells. Nature, 2021. 591(7851): p. 620-626.
12. Hashmi, A., et al., Cell-state transitions and collective cell movement generate an endoderm-like region in gastruloids. Elife, 2022. 11.
13. Cermola, F., et al., Stabilization of cell-cell adhesions prevents symmetry breaking and locks in pluripotency in 3D gastruloids. Stem Cell Reports, 2022. 17(11): p. 2548-2564.
14. D'Aniello, C., et al., Collagen Prolyl Hydroxylation-Dependent Metabolic Perturbation Governs Epigenetic Remodeling and Mesenchymal Transition in Pluripotent and Cancer Cells. Cancer Res, 2019. 79(13): p. 3235-3250.
15. D'Aniello, C., et al., A novel autoregulatory loop between the Gcn2-Atf4 pathway and (L)-Proline [corrected] metabolism controls stem cell identity. Cell Death Differ, 2015. 22(7): p. 1094-105.
16. Comes, S., et al., L-Proline induces a mesenchymal-like invasive program in embryonic stem cells by remodeling H3K9 and H3K36 methylation. Stem Cell Reports, 2013. 1(4): p. 307-21.
17. D'Aniello, C., et al., Collagen prolyl hydroxylation-dependent metabolic perturbation governs epigenetic remodeling and mesenchymal transition in pluripotent and cancer cells. Cancer Res, 2019.
18. Cermola, F., et al., Gastruloid Development Competence Discriminates Different States of Pluripotency. Stem Cell Reports, 2021. 16(2): p. 354-369.
19. Cermola, F., E.J. Patriarca, and G. Minchiotti, Generation of Gastruloids from Epiblast-Like Cells. Methods Mol Biol, 2022. 2490: p. 197-204.
20. Baillie-Johnson, P., et al., Generation of Aggregates of Mouse Embryonic Stem Cells that Show Symmetry Breaking, Polarization and Emergent Collective Behaviour In Vitro. J Vis Exp, 2015(105).